

Article

Exploring the Use of Pattern Classification Approaches for the Recognition of Landslide-Triggering Rainfalls

Ascanio Rosi 

Department of Geosciences, University of Padova, 35131 Padova, Italy; ascanio.rosi@unipd.it

Abstract: Rainfall-triggered landslides are well-known natural hazards that pose significant risks, and lot of effort has been invested to reduce the risk associated with this type of phenomenon. One approach to reduce such risk is the establishment of landslide early warning systems (LEWSs). LEWSs are designed to proactively identify conditions favorable to the initiation of landslides. When dealing with regional scale works, LEWSs are usually based on statistical methodologies to determine the minimum amount of rainfall required to trigger a landslide. This amount is often expressed in terms of minimum intensity or cumulative rainfall in a given time period. This research explores the use of artificial intelligence, specifically Long Short-Term Memory (LSTM) networks to analyze rainfall time series as either likely or not likely to result in a landslide. Various lengths of time series and different configurations of the model were tested to identify the best setting of the model. To develop the research, the selected test site was the Emilia-Romagna region in Italy, which has a robust landslide inventory, with assessed accuracy. Model performances were evaluated using several statistical indicators, including sensitivity (0.9), specificity (0.8), positive prediction power (0.82), negative prediction power (0.89), Efficiency (0.85) and misclassification rate (0.15). These results showed that the defined model correctly identified the rainfall conditions associated with landslide initiation with a high degree of accuracy and a low rate of false positives. In summary, this research demonstrates the potential of artificial intelligence, particularly LSTM networks, in improving the accuracy of LEWSs by analyzing rainfall time series data, ultimately enhancing our ability to predict and mitigate the risks of rainfall-triggered landslides.



check for updates

Citation: Rosi, A. Exploring the Use of Pattern Classification Approaches for the Recognition of Landslide-Triggering Rainfalls. *Sustainability* **2023**, *15*, 15145. <https://doi.org/10.3390/su152015145>

Academic Editors: Guoqing Chen and Peng Tang

Received: 31 August 2023

Revised: 6 October 2023

Accepted: 19 October 2023

Published: 23 October 2023



Copyright: © 2023 by the author. Licensee MDPI, Basel, Switzerland. This article is an open access article distributed under the terms and conditions of the Creative Commons Attribution (CC BY) license (<https://creativecommons.org/licenses/by/4.0/>).

Keywords: landslide; rainfall; LSTM; machine learning; LEWS

1. Introduction

Rainfall-triggered landslides are widely recognized natural hazards that annually incurs economic and social losses. To address the risk associated with these phenomena on a regional scale, the establishment of Landslide Early Warning Systems (LEWSs) is a commonly employed strategy. These systems are designed to predict the onset of landslides by monitoring rainfall conditions associated with their initiation. Commonly adopted methodologies involve the use of statistical approaches for the definition of rainfall thresholds, which can be constructed using factors such as rainfall duration and intensity or cumulative rainfall [1–3], and they can be coupled with antecedent rainfall [4–6] or soil moisture data [7–9]. These approaches have proven to be reliable, but they still face a degree of uncertainty, often stemming from the presence of a relevant number of false alarms [6].

In addition to statistical approaches, deterministic models [10–12] can provide robust results, as they rely on well-established physical principles governing slope behavior. However, their application over large areas remains constrained due to several factors. One significant limitation is the substantial number of parameters these models require. Collecting these parameters with a high level of accuracy at the basin or regional scale can be a formidable challenge. Consequently, the utilization of deterministic models is predominantly restricted to analyzing single slopes or small river basins.

In recent years, artificial intelligence (AI) has made its way into various scientific disciplines, proving to be a powerful tool to solve complex tasks. Within the field of landslide hazard assessment, AI has been successfully used for several tasks [13], including landslide susceptibility mapping [14–17], landslide detection [18–21] and monitoring [22], while more recently, attempts have been made to use AI for forecasting landslide-triggering conditions [23–26].

Among the various AI methodologies, pattern recognition is used to discern patterns and regularities within datasets and finds applications in diverse domains, such as the recognition of images, objects, faces or fingerprints. Pattern recognition can be also used for voice and sound classification, for instance, associating a recording with a specific speaker. The classification of voices involves identifying sound patterns within recordings of a given length, where the voice amplitude varies over the time.

This work aims to explore the potential of using the pattern recognition methodology to classify rainfall time series (where rainfall intensity varies over the time) that may or may not be associated with landslide triggers. Specifically, the Long Short-Term Memory (LSTM) model was employed. LSTM represents an advanced iteration of the Recurrent Neural Network (RNN) and excels at capturing and retaining both long- and short-term dependencies within data. This capability addresses the vanishing gradient problem often encountered in traditional RNNs and reduces backpropagation errors [27,28].

In contrast to conventional methods for identifying landslide-triggering rainfall conditions, which primarily focus on parameters like minimum rainfall intensity, cumulative rainfall, antecedent rainfall and duration, this study takes a different approach. It leverages LSTM to consider the entire rainfall pattern of an event, thereby exploring its potential for identifying rainfall patterns that trigger landslides. To develop an effective voice classification model, an adequate number of voice recordings are needed for each class, and each recording should have a sufficient length. Similarly, for accurate classification of rain events, an initial definition of the number of records (and their length) to associate with a landslide or with a no-landslide event is needed, as well as the tuning of the parameters of the AI model. As this study represents a pioneering attempt in applying pattern recognition to rainfall time series analysis, there is currently a scarcity of existing literature for comparison. In light of this, the Emilia Romagna region of Italy was used as a test site, where a good knowledge of the landslide phenomenon is present and where a landslide warning system based on statistical rainfall threshold exists. This choice was made to have a reliable landslide dataset to evaluate the AI model and to have some previously validated results to be used as a benchmark for this work.

2. Material and Methods

2.1. Test Site Description

The selected test site is Emilia Romagna region, located in the northern part of Italy (Figure 1). This test site was selected since a large landslide inventory is available. Notably, this inventory has been subjected to prior research activities [6,8,29], which have optimized its quality and relevance. This solid database forms a strong foundation for the current study. In this area, a warning system based on rainfall threshold is available [30], so it can be used for a comparison with the outcomes of this work. A dense rainfall network, with hourly recordings, is available as well.

From a geological standpoint, the southwestern part of the study area predominantly comprises arenaceous flysch formations with mountains up to 2000 m, that downgrade in a northeast direction, where wide plains and alluvial deposits are present. Rainfall distribution follows a similar pattern, with higher mean annual precipitation in the southwestern part of the region (ca. 2000 mm/year) and lower values towards northeast.

2.2. Landslide Inventory and Rainfall Data

For this research, the landslide inventory created by the regional Geological, Seismic and Soil Service, previously utilized in other studies [6], was selected as the primary dataset. The inventory included detailed information, associating each landslide event with data

about the precision of location and date; this allowed the extraction of 1090 landslides, for which both the exact triggering date and precise location were known, to be used to train the AI model. Less accurate data were not used to avoid introducing uncertainties within the model, although these less accurate records were considered when verifying the results. The landslide events covered the period from 2005 to 2015.

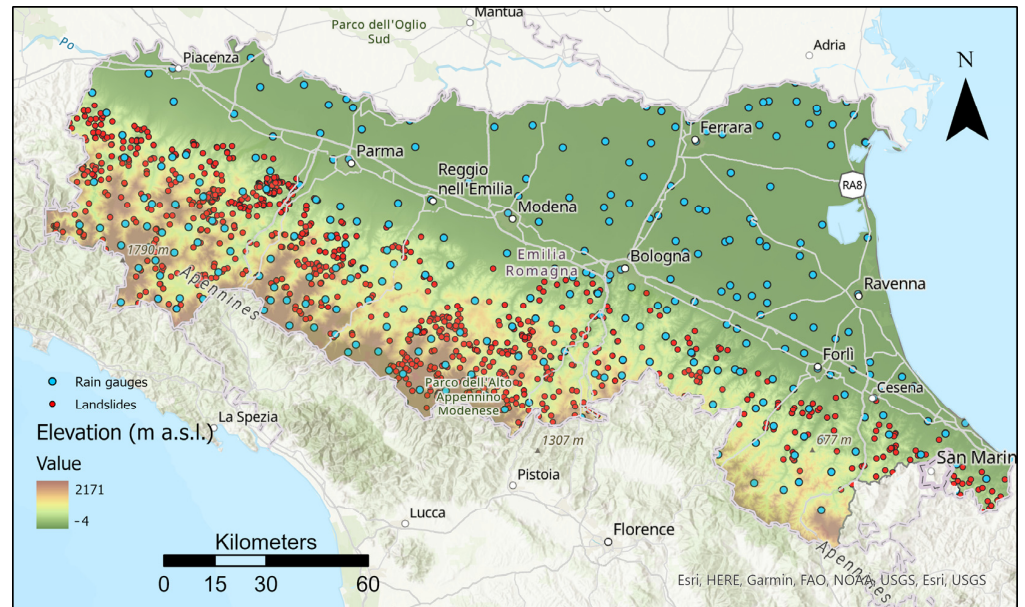


Figure 1. Map of the study area.

The highest number of landslides was recorded in 2009, while 2012, 2013 and 2014 had fewer landslides with accurate descriptions (Figure 2). Most landslides occurred between November and April, which is the rainiest season in the region, while fewer landslides have been recorded during the summer, when less rainfall is usually recorded.

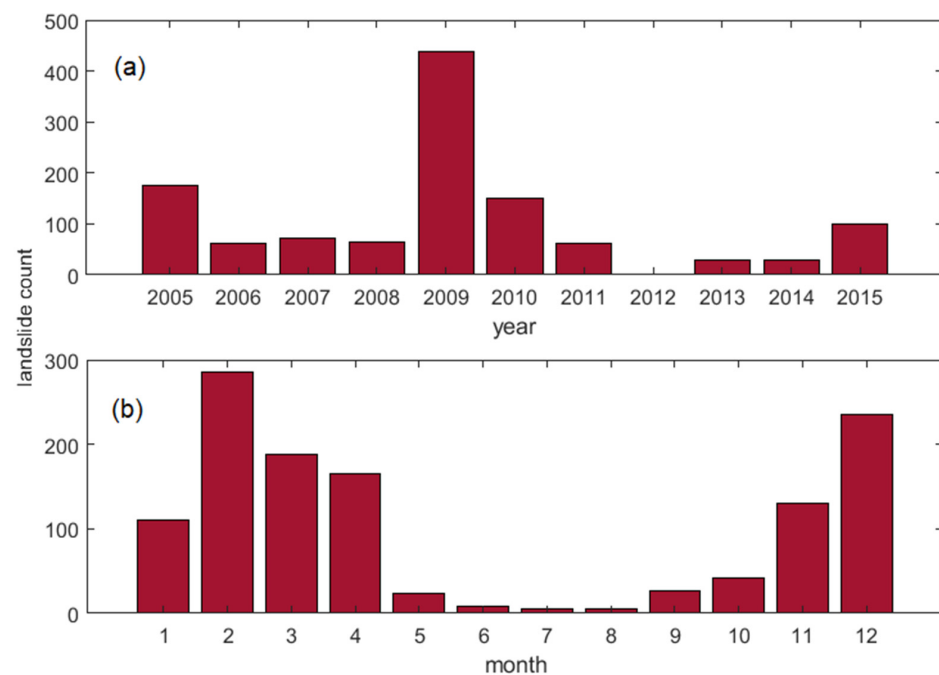


Figure 2. Landslide distribution over the period of analysis: (a) annual distribution, (b) monthly distribution.

Rainfall data were gathered from a dense network of rain gauges made up of about 300 stations distributed across the region (Figure 1). To develop this research, hourly rainfall data were used.

2.3. Methodology

As described in the introduction, this work is aimed at the evaluation of the use of pattern recognition approaches to identify and properly classify the rainfall conditions that can trigger a landslide. The selection of the most appropriate AI model was the first step of the work. Given that rainfall records are sequential time series data, it was decided to use Long Short-term Memory (LSTM), a deep learning methodology that has a track record of effectively handling sequential data and capturing both short-term and long-term dependencies between different time steps [31,32]. At the beginning, each landslide was associated with the closest rain gauge, and the hourly rainfall data of the 60 days preceding each landslide were extracted; a total of 1090 rainfall time series that triggered landslide were hence created. A number of time series not associated with landslide initiation was also extracted; in this case twice as much as previous data were extracted, to account for incomplete time series, that were then discarded. Each time series was labeled with "1" if associated with a landslide or "0" if not. To minimize data uncertainties for non-landslide events, a specific 4-day period around each landslide event (2 days before and 2 days after) was defined, during which rain data not associated with landslides were excluded from the training dataset.

The length of rainfall times series was initially set to 60 days (1440 h), but this choice posed several problems, including difficulty in finding complete time series of this length and excessive computational load. After an in-depth analysis of previous works in the same study area [6,8,30,33], five time intervals were selected to perform the analyses: 3, 7, 10, 15 and 30 days.

Similar to AI models for voice classification that require multiple recordings for each class (e.g., to distinguish between different speakers, multiple speech records are needed for each one to train the model), determining the best number of rainfall records to associate to each landslide or no-landslide class was necessary.

Since it was not possible to define a priori the best number of rainfall records to use for each class, an iterative procedure was set up, starting from 1 recording for each label and increasing up to 10.

In the case of the association with 1 record, each event (both labeled 1 or 0) was used independently to train the model, while with the increase in the number of tracks, events were grouped into small batches with the same labels; for example, using 5 tracks, several groups of rainfall events (each of them with 5 records) associated or not with the triggering of landslides were created and used to perform the analyses (Figure 3). Rainfall time series were then divided into three sets: training set (70% of the data), test set (20% of the data) and validation set (10% of the data); each set was equally balanced between landslide and no-landslide events.

The LSTM model underwent ten cycles of train/test/validation for each configuration (the number of rainfall records). In each cycle, the rainfall records were grouped differently (same number of records for each batch, but with different rainfall series), and the accuracy of the model was evaluated in each cycle. This iterative process allowed verifying the stability of model with the given data and configuration, while accuracy values were used to identify the best configuration. The choice of randomly grouping the rainfall records in each batch for each iteration prevented the overweighting of the areas with more landslide (this would happen if rainfall records were grouped on the basis of the spatial location), hence avoiding the biasing or overfitting of the model (changing the data in each batch every time avoided that the model was over-adapted to specific groups of time series). This approach was consistently applied across all selected time intervals to maintain the integrity and robustness of the model throughout the research.

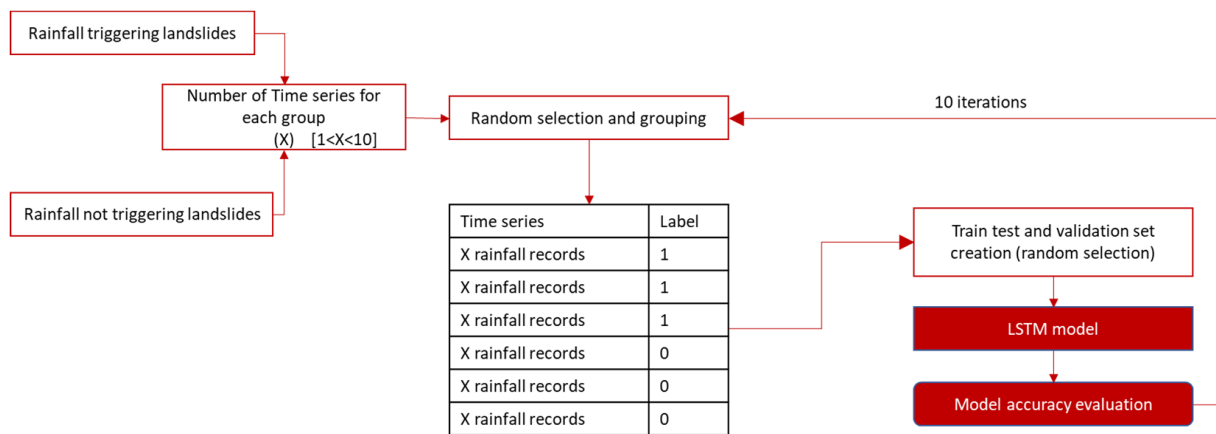


Figure 3. Flow chart of the data processing chain. The whole procedure was repeated for rainfall at intervals of 3, 10, 15 and 30 days.

Since the work was focused on the possibility of using this kind of model for landslide triggering, after an initial optimization of the key parameters (e.g., the number of layers of the model), the configuration of the LSTM was kept as simple and consistent as possible throughout the iterations to ensure comparability. More specifically, the model was set up to work with Adam solver, a fully connected layer, a SoftMax layer and a classification layer.

This approach of maintaining a consistent model configuration allowed for a clear evaluation of the impact of changes in other aspects of the analysis, such as the number of rainfall records or the time intervals, while keeping the core model structure constant.

3. Results

3.1. Model Configuration

Following the procedure outlined in the previous section, it was possible to identify the optimal configuration of the LSTM model, in terms of number of rain records considered in each group. The box plots of accuracy estimation for each model configuration are reported in Figure 4.

The use of all rain records independently (1 rain gauge) resulted in the poorest performance, in terms of both mean and variability of accuracy values, across all of the analyzed time intervals.

Conversely, superior results were obtained when a larger number of rainfall records were grouped together, leading to higher accuracy and reduced variability. The performances of the model did exhibit significant improvement when using five or more rain records in each group. The configuration with five records was therefore selected as the best choice, striking a balance between accuracy and computational efficiency.

3.2. Model Performance

The selected configuration underwent a more in-depth evaluation of the performances using several statistical indexes as the receiver operating characteristic (ROC) curve, sensitivity, specificity, positive prediction power and negative prediction power.

The ROC curve showed an area under the ROC curve (AUC) value of 0.9 (Figure 5), indicating a satisfactory performance of the model. Such a high value can indicate the presence of an overfitting issue, but this evidence can be discarded, since several precautions were taken to avoid this problem, as described in the previous section.

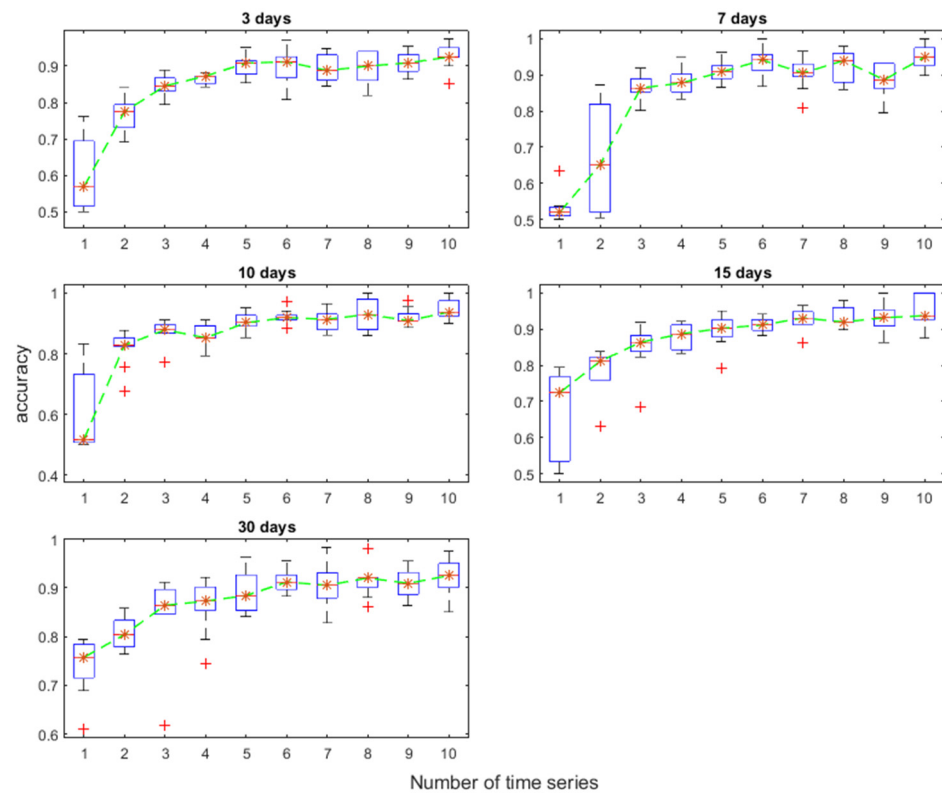


Figure 4. Boxplots showing the evaluation of the efficiency of each model configuration. Each panel represents the result for a different time interval using from 1 to 10 time series. Asterisks represent the median value of accuracy of each configuration, red crosses represent the outliers.

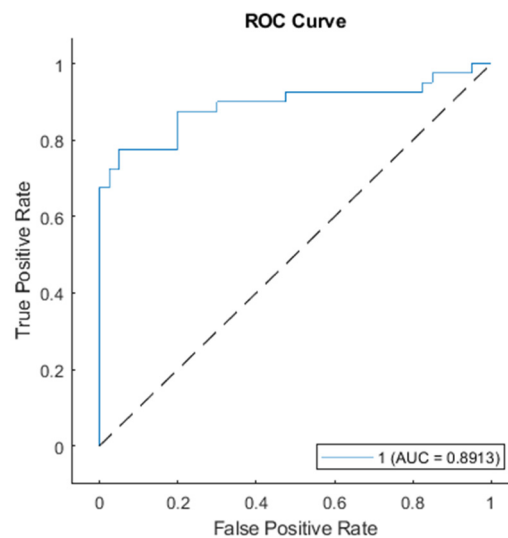


Figure 5. ROC curve of the model and AUC value.

The statistical indexes (Table 1) confirmed the good performance of the model.

Table 1. Statistical indexes used to evaluate the performance of the selected model.

Index	Se	Sp	PPP	NPP	E	Misclassification Rate
Value	0.9	0.8	0.82	0.89	0.85	0.15

Sensitivity (Se) represents the ability of the model to properly classify rainfall that triggers landslides. It is defined as the ratio between the true positive (TP) predictions

(i.e., the number of landslides correctly predicted by the model) and the number of total positive (i.e., number of landslide events, both predicted (TP) and unpredicted (FN)); the sensitivity value of the model is 0.9, meaning that the model correctly predicted 90% of the events. The formula for sensitivity is:

$$Se = TP / (TP + FN)$$

Specificity (Sp) shows ability to properly classify rainfalls that did not trigger landslides and is calculated as the ratio between true negatives (TN, the number of rainfalls not linked to landslide that the model correctly identified) and the total number of rainfalls that did not trigger landslides; the model achieved a score of 0.8, meaning that 80% of rainfall that did not trigger landslides was correctly identified. The equation for specificity is:

$$Sp = TN / (TN + FP)$$

Positive prediction power (PPP) is the probability of correctly classifying a rainfall that triggered landslides and is defined as the ratio between true positives and all positive predictions (as the sum of true positives and false positives (FP)); the model showed a PPP of 0.82, meaning that the 82% of all the events identified as potentially landslide-triggering, actually triggered a landslide. PPP is calculated as:

$$PPP = TP / (TP + FP)$$

Negative prediction power (NPP) indicates the probability of correctly classifying rainfall that did not trigger landslides and is calculated as the ratio between the number of true negatives and all negative predictions (as the sum of true and false negatives); the model achieved a score of 0.89, hence 89% of the events classified as not capable of triggering landslides was correctly identified. The equation for NPP is:

$$NPP = TN / (TN + FN)$$

Efficiency (E) represents the number of good predictions (both for landslide-triggering and non-triggering events) over the total number of events; the score of 0.85 indicates that globally, the model correctly classified 85% of all rain events. Efficiency is calculated as:

$$E = (TP + TN) / (TP + FP + TN + FN)$$

Misclassification (M) rate (as the number of wrong predictions over the total number of events) was 0.15, based on the equation:

$$M = (FP + FN) / (TP + FP + TN + FN)$$

4. Model Validation and Operational Simulation

Besides the validation made in the training process, a more accurate validation) was performed, by using a completely independent event not used in the model development. The validation was also used to simulate how this kind of model can be potentially used inside a LEWS. To achieve this goal, a period with several landslides was selected. The model was set up to make predictions every hour, to verify its ability to identify the rain conditions associated with landslide initiation.

This experiment was designed to test the model's performance under challenging conditions. It focused on a period with numerous landslide events scattered across the study area, occurring on different dates. However, rainfall data were collected from only five rain gauges situated close to a specific area affected by some landslides, referred to as the "target area". This experiment was also designed to assess whether the model could effectively identify only the landslides occurring near the rain gauges, while refraining from issuing false predictions for landslide events outside the target area. This experiment

also allowed verifying the model behavior in such a noisy scenario, with rain events that triggered landslides in other zones, outside the target area.

The selected period spanned from 10 March 2011 to 30 March 2011; during this interval, the target zone (Figure 6) experienced landslide events on days 14, 15, 16, 17, 18 and 29, while landslides in different areas were reported on days 10, 12, 14, 15, 16 and 21.

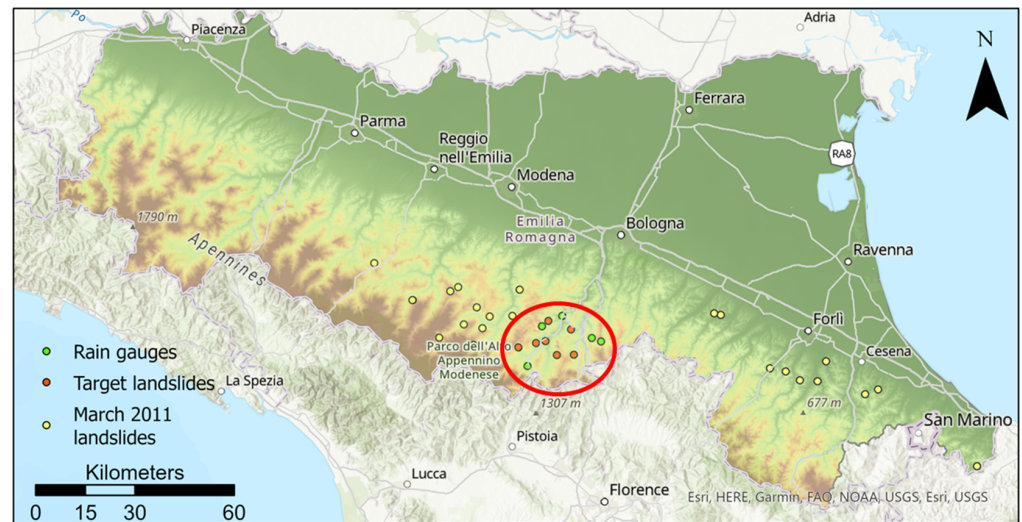


Figure 6. Distribution of landslides in March 2011; the red circle indicates the target area.

As previously mentioned, the model was configured to make predictions on an hourly basis, taking into account the rainfall recorded during the 72 h preceding each prediction. In total, 504 predictions were generated based on this setup, allowing for a detailed assessment of the model's performance and its ability to provide timely warnings of potential landslide events.

Results showed very low values of landslide probability (below 0.1) from the beginning of the simulation until 13 March at 15:00 h, when the probability values increased to 0.82 and subsequently to 0.9 in the following hours. This period of increased probability correctly anticipated a landslide event. The landslide probability remained close to 1 until 19 March at 10:00 h. During this time, the model effectively predicted landslide events. Then the landslide probability dropped back close to 0 until 28 March at 09:00 h, when it increased to 0.78 and close to 1 in the subsequent hours; then it remained constant (close to 1) until the end of 30 March, that is the end of the simulation (Figure 7).

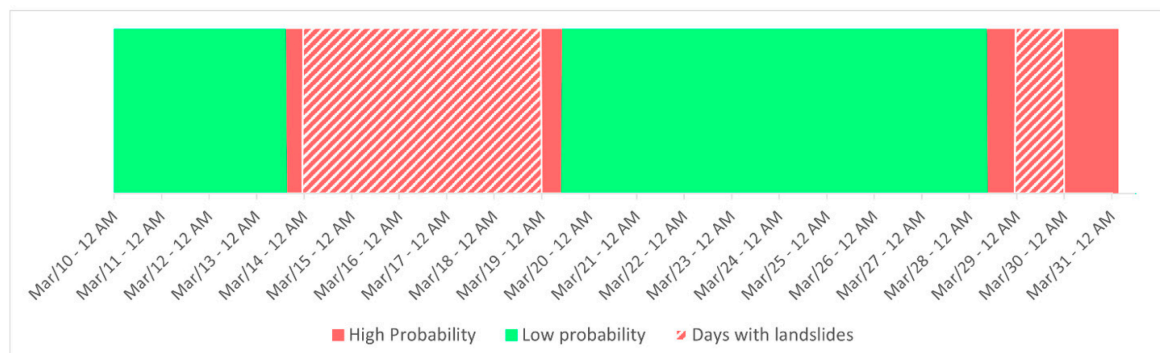


Figure 7. Schematic representing the temporal distribution of landslide probabilities over the validation period. Green represents the periods in which the model predicted low landslide probability, red indicates periods with prediction of high landslide probability, and white stripes indicate the days with landslides.

According to the results, the model correctly predicted the landslide events between 14 and 19 March as well as the event of 29 March, and the rainfall that triggered landslides outside the focus area on days 10, 12 and 21 did not influence the model outputs. The first time the model issued a high landslide probability was in 13 March at 11:00 h, and the first landslide was reported on the following day, so this can be considered a good prediction. The landslide probability dropped back to low values the morning after the landslide reported on 18 March. For the landslide of 29 March, the model raised the probability value the morning before, but it remained at high values even on the day after the landslide.

5. Discussion

This research has focused on investigating the applicability of pattern recognition to identify rainfalls that could potentially trigger landslides. In an effort to mitigate uncertainties associated with the input data, the work was conducted in an area where a robust and reliable landslide inventory and previous studies on landslides [6,8,30,33] were available; those studies have been considered as references to start this work.

To train the LSTM model, only landslides with verified dates and precise locations were used, thereby preventing the introduction of incorrect or uncertain data into the model. The LSTM model was trained with various configurations, experimenting with different combinations of rainfall time series length and the number of rainfall records used within each group of series. The configuration that consistently delivered the best results meeting the criteria of high accuracy and stability (low variation in accuracy across different data combinations while using shorter time series, was selected as the optimal configuration.

The best performing model used three-day rainfalls, with groups of five rain gauges. This model resulted in an AUC value of 0.89, with a sensitivity of 0.9 and a PPP of 0.82, indicating its capability to correctly identify 90% of all landslides and that 82% of all rainfalls classified as potentially landslide-triggering were correct. To put these results into context, a comparison with previous researches in the same study area was made.

The work of Martelloni et al. [30], based on a statistical approach, achieved a sensitivity of 0.73 and a PPP of 0.17, while the rainfall thresholds (intensity–duration) defined by Rosi et al. [6] had sensitivity values ranging from 0.74 to 0.99 (average 0.91) and a PPP ranging from 0.40 to 0.80 (average 0.55). This comparison indicates that the LSTM model has a general capability of identifying landslides (based on sensitivity values) higher than the work of Martelloni et al. [30] and similar to the work of Rosi et al. [6], but LSTM outperformed in terms of PPP values, that are significantly higher than those in the other works. This means that the LSTM model has higher precision in defining the rainfall conditions that can trigger landslides. In an operative use, this means that the model offers a high rate of correct predictions, with a low number of false predictions (events classified as potentially landslide-triggering that did not result in a landslide). Therefore, the LSTM model can be considered a valuable method in identifying landslide-triggering conditions while minimizing the instances where it predicts landslides incorrectly.

While the results of this work indicated the potential of pattern recognition in landslide forecasting, there are some important considerations to address before implementing it for operational use, such as in a LEWS.

First, the study area is well known by the author, and the quality of the landslide inventory was already assessed. To ensure the reliability and applicability of the model in regions with different climatic and geological settings, further testing should be conducted in diverse geographic areas. Larger landslide inventories, covering wider areas with more complex environments should be tested as well, to verify the behavior of the model. Additionally, working with larger inventories may help develop a model that does not require the creation of groups of time series to identify the rain paths that can (or cannot) trigger a landslide, potentially simplifying the forecasting process.

This will be helpful in increasing the spatial resolution of the predictions, since the presented model relies on the use of five rain gauges each time, which leads to a quite coarse spatial resolution. Furthermore, in areas with a low density of rain gauges (Emilia

Romagna was also selected because it has a dense rain gauge network), the applicability of the model should be tested. This will help determine its effectiveness in areas with limited data availability and lower spatial coverage. It may require adaptations or enhancements to account for the sparse data, ensuring that the model maintains its accuracy and reliability in such environments.

6. Conclusions

This study applied pattern recognition methodology to rainfall time series for the purpose of forecasting rainfall-induced landslides. The test site was the Emilia Romagna region, where a landslide inventory of 1090 landslides from 2005 to 2015 with verified locations and dates was available, along with a dense rain gauge network. The identification of the most relevant durations of rainfall time series was initially based on literature works and further refined by analyzing the performances of the LSTM model with different durations. Multiple configurations of the LSTM model were tested, involving random grouping of the data and repeating the training-and-testing procedure several times, to identify the most effective model. The selected model had a high AUC value (0.89), as well as high values of sensitivity and PPP, indicating its capability to properly identify rainfalls events that can trigger landslides, while maintaining a low rate of false predictions (about 18%).

One of the primary advantages of this model is its high temporal resolution, as it was tested to make hourly predictions for a period of 20 days. However, it has limitations in terms of spatial resolution, as it is not capable of accurately pinpointing the location of the landslides. Additionally, further experiments with larger landslide inventories and in different environments are required to verify its exportability.

In the future, this type of model has the potential to be integrated with landslide hazard maps (as susceptibility maps) to better identify areas where landslides can trigger. This integration could lead to a more accurate landslide forecasting model, ultimately improving the early warning and mitigation of landslide-related risks.

Funding: This research received no external funding.

Institutional Review Board Statement: Not applicable.

Informed Consent Statement: Not applicable.

Data Availability Statement: Used data can be download from the web pages of public authorities of Emilia Romagna Region. Landslide data: <https://ambiente.regione.emilia-romagna.it/it/geologia/geologia/dissesto-idrogeologico/larchivio-storico-dei-movimenti-franosi>. Rainfall data: <https://simc.arpae.it/dext3r/>.

Conflicts of Interest: The author declares no conflict of interest.

References

1. Baum, R.L.; Godt, J.W. Early Warning of Rainfall-Induced Shallow Landslides and Debris Flows in the USA. *Landslides* **2010**, *7*, 259–272. [[CrossRef](#)]
2. Dikshit, A.; Satyam, N.; Pradhan, B. Estimation of Rainfall-Induced Landslides Using the TRIGRS Model. *Earth Syst. Environ.* **2019**, *3*, 575–584. [[CrossRef](#)]
3. Peruccacci, S.; Brunetti, M.T.; Gariano, S.L.; Melillo, M.; Rossi, M.; Guzzetti, F. Rainfall Thresholds for Possible Landslide Occurrence in Italy. *Geomorphology* **2017**, *290*, 39–57. [[CrossRef](#)]
4. Aleotti, P. A Warning System for Rainfall-Induced Shallow Failures. *Eng. Geol.* **2004**, *73*, 247–265. [[CrossRef](#)]
5. Kim, S.W.; Chun, K.W.; Kim, M.; Catani, F.; Choi, B.; Seo, J.I. Effect of Antecedent Rainfall Conditions and Their Variations on Shallow Landslide-Triggering Rainfall Thresholds in South Korea. *Landslides* **2021**, *18*, 569–582. [[CrossRef](#)]
6. Rosi, A.; Segoni, S.; Canavesi, V.; Monni, A.; Gallucci, A.; Casagli, N. Definition of 3D Rainfall Thresholds to Increase Operative Landslide Early Warning System Performances. *Landslides* **2021**, *18*, 1045–1057. [[CrossRef](#)]
7. Abraham, M.; Satyam, N.; Rosi, A.; Pradhan, B.; Segoni, S. Usage of Antecedent Soil Moisture for Improving the Performance of Rainfall Thresholds for Landslide Early Warning. *Catena* **2021**, *200*, 105147. [[CrossRef](#)]

8. Segoni, S.; Rosi, A.; Lagomarsino, D.; Fanti, R.; Casagli, N. Brief Communication: Using Averaged Soil Moisture Estimates to Improve the Performances of a Regional-Scale Landslide Early Warning System. *Nat. Hazards Earth Syst. Sci.* **2018**, *18*, 807–812. [[CrossRef](#)]
9. Wicki, A.; Lehmann, P.; Hauck, C.; Seneviratne, S.I.; Waldner, P.; Stähli, M. Assessing the Potential of Soil Moisture Measurements for Regional Landslide Early Warning. *Landslides* **2020**, *17*, 1881–1896. [[CrossRef](#)]
10. Rossi, G.; Catani, F.; Leoni, L.; Segoni, S.; Tofani, V. HIRESS: A Physically Based Slope Stability Simulator for HPC Applications. *Nat. Hazards Earth Syst. Sci.* **2013**, *13*, 151–166. [[CrossRef](#)]
11. Alvioli, M.; Baum, R.L. Parallelization of the TRIGRS Model for Rainfall-Induced Landslides Using the Message Passing Interface. *Environ. Model. Softw.* **2016**, *81*, 122–135. [[CrossRef](#)]
12. Masi, E.B.; Tofani, V.; Rossi, G.; Cuomo, S.; Wu, W.; Salciarini, D.; Caporali, E.; Catani, F. Effects of roots cohesion on regional distributed slope stability modelling. *Catena* **2023**, *222*, 106853. [[CrossRef](#)]
13. Ma, Z.; Mei, G.; Piccialli, F. Machine Learning for Landslides Prevention: A Survey. *Neural Comput. Appl.* **2021**, *33*, 10881–10907. [[CrossRef](#)]
14. Azarafza, M.; Azarafza, M.; Akgün, H.; Atkinson, P.M.; Derakhshani, R. Deep Learning-Based Landslide Susceptibility Mapping. *Sci. Rep.* **2021**, *11*, 24112. [[CrossRef](#)]
15. Camera, C.A.; Bajni, G.; Corno, I.; Raffa, M.; Stevenazzi, S.; Apuani, T. Introducing Intense Rainfall and Snowmelt Variables to Implement a Process-Related Non-Stationary Shallow Landslide Susceptibility Analysis. *Sci. Total Environ.* **2021**, *786*, 147360. [[CrossRef](#)]
16. Sur, U.; Singh, P.; Meena, S.R. Landslide susceptibility assessment in a lesser Himalayan road corridor (India) applying fuzzy AHP technique and earth-observation data. *Geomat. Nat. Hazards Risk* **2020**, *11*, 2176–2209. [[CrossRef](#)]
17. Huang, Y.; Zhao, L. Review on Landslide Susceptibility Mapping Using Support Vector Machines. *Catena* **2018**, *165*, 520–529. [[CrossRef](#)]
18. Bhuyan, K.; Tanyaş, H.; Nava, L.; Puliero, S.; Meena, S.R.; Floris, M.; van Westen, C.; Catani, F. Generating Multi-Temporal Landslide Inventories through a General Deep Transfer Learning Strategy Using HR EO Data. *Sci. Rep.* **2023**, *13*, 162. [[CrossRef](#)]
19. Ghorbanzadeh, O.; Blaschke, T.; Gholamnia, K.; Meena, S.R.; Tiede, D.; Aryal, J. Evaluation of Different Machine Learning Methods and Deep-Learning Convolutional Neural Networks for Landslide Detection. *Remote Sens.* **2019**, *11*, 196. [[CrossRef](#)]
20. Nava, L.; Monserrat, O.; Catani, F. Improving Landslide Detection on SAR Data through Deep Learning. *IEEE Geosci. Remote Sens. Lett.* **2022**, *19*, 1–5. [[CrossRef](#)]
21. Pradhan, B.; Seeni, M.I.; Nampak, H. Integration of LiDAR and QuickBird Data for Automatic Landslide Detection Using Object-Based Analysis and Random Forests. In *Laser Scanning Applications in Landslide Assessment*; Pradhan, B., Ed.; Springer International Publishing: Cham, Switzerland, 2017; pp. 69–81. [[CrossRef](#)]
22. Chae, B.-G.; Park, H.-J.; Catani, F.; Simoni, A.; Berti, M. Landslide Prediction, Monitoring and Early Warning: A Concise Review of State-of-the-Art. *Geosci. J.* **2017**, *21*, 1033–1070. [[CrossRef](#)]
23. Collini, E.; Palesi, L.A.I.; Nesi, P.; Pantaleo, G.; Nocentini, N.; Rosi, A. Predicting and Understanding Landslide Events with Explainable AI. *IEEE Access* **2022**, *10*, 31175–31189. [[CrossRef](#)]
24. Distefano, P.; Peres, D.J.; Scandura, P.; Cancelliere, A. Brief Communication: Introducing Rainfall Thresholds for Landslide Triggering Based on Artificial Neural Networks. *Nat. Hazards Earth Syst. Sci.* **2022**, *22*, 1151–1157. [[CrossRef](#)]
25. Mondini, A.C.; Guzzetti, F.; Melillo, M. Deep Learning Forecast of Rainfall-Induced Shallow Landslides. *Nat. Commun.* **2023**, *14*, 2466. [[CrossRef](#)] [[PubMed](#)]
26. Nocentini, N.; Rosi, A.; Segoni, S.; Fanti, R. Towards Landslide Space-Time Forecasting through Machine Learning: The Influence of Rainfall Parameters and Model Setting. *Front. Earth Sci.* **2023**, *11*, 1152130. [[CrossRef](#)]
27. Hochreiter, S.; Schmidhuber, J. Long short-term memory. *Neural Comput.* **1997**, *9*, 1735–1780. [[CrossRef](#)]
28. Abed, M.; Imteaz, M.A.; Ahmed, A.N.; Huang, Y.F. A novel application of transformer neural network (TNN) for estimating pan evaporation rate. *Appl. Water Sci.* **2023**, *13*, 31. [[CrossRef](#)]
29. Segoni, S.; Rosi, A.; Fanti, R.; Gallucci, A.; Monni, A.; Casagli, N. A Regional-Scale Landslide Warning System Based on 20 Years of Operational Experience. *Water* **2018**, *10*, 1297. [[CrossRef](#)]
30. Martelloni, G.; Segoni, S.; Fanti, R.; Catani, F. Rainfall Thresholds for the Forecasting of Landslide Occurrence at Regional Scale. *Landslides* **2012**, *9*, 485–495. [[CrossRef](#)]
31. Karim, F.; Majumdar, S.; Darabi, H.; Chen, S. LSTM Fully Convolutional Networks for Time Series Classification. *IEEE Access* **2017**, *6*, 1662–1669. [[CrossRef](#)]
32. Yu, Y.; Zeng, X.; Xue, X.; Ma, J. LSTM-Based Intrusion Detection System for VANETs: A Time Series Classification Approach to False Message Detection. *IEEE Trans. Intell. Transp. Syst.* **2022**, *23*, 23906–23918. [[CrossRef](#)]
33. Berti, M.; Martina, M.; Franceschini, S.; Pignone, S.; Simoni, A.; Pizziolo, M. Probabilistic Rainfall Thresholds for Landslide Occurrence Using a Bayesian Approach. *J. Geophys. Res. Earth Surf.* **2012**, *117*, F04006. [[CrossRef](#)]

Disclaimer/Publisher's Note: The statements, opinions and data contained in all publications are solely those of the individual author(s) and contributor(s) and not of MDPI and/or the editor(s). MDPI and/or the editor(s) disclaim responsibility for any injury to people or property resulting from any ideas, methods, instructions or products referred to in the content.